Kragujevac J. Sci. 43 (2021) 5-14. UDC 537.63:546.171.1
Original scientific paper

THE EFFECT OF MAGNETIC FIELD ON THE TUNNELING YIELD OF AMMONIA MOLECULES

Violeta M. Petrović[1], Hristina S. Delibašić[1]*, Ivan D. Petrović[2]

[1]*University of Kragujevac, Faculty of Science, Department of Physics, Radoja Domanovića 12, 34000 Kragujevac, Serbia*
[2]*Academy of Professional Studies Šumadija, Department in Kragujevac, Kosovska 8, 34000 Kragujevac, Serbia*
*****Corresponding author; E-mail: hristina.delibasic@pmf.kg.ac.rs

(Received February 02, 2021; Accepted April 29, 2021)

ABSTRACT. We analyzed the influence of magnetic component of the laser field on the tunneling yield, in a strong near-relativistic field for a squared hyperbolic secant pulse distribution. The obtained results indicate that the inclusion of the magnetic component is necessary in the observed regime.

Keywords: ammonia molecule, magnetic field, tunneling yield.

INTRODUCTION

Photoionization of atoms and molecules is the initial step of many interesting strong-field phenomena such as electron recollision and nonsequential double ionization (NDI) (LI *et al.*, 2020), molecular imaging by the recolliding electrons (MIRE) (PENG *et al.*, 2019), high-order above-threshold ionization (HATI) (BRENNECKE and LEIN, 2018), high-order harmonic generation (HHG) (BRAY *et al.*, 2019). Additionally, the electrons emitted by photoionization contain structural information suitable for orbital imaging (YUAN *et al.*, 2017; CHANG *et al.*, 2019) and nuclear dynamics, as well (ARNOLD *et al.*, 2017). Because of all above mentioned, the ionization mechanism depending on the laser parameters, such as intensity, power, frequency, and wavelength has attracted considerable interests of both experimental and theoretical groups. The goal was to obtain an accurate theoretical model of atoms and molecules photoionization processes and as a result, multiple theoretical approaches (KELDYSH, 1965; KRAINOV, 1997; ZHAO *et al.*, 2014) have been developed. In this paper we are interested in those which are dealing with molecules that are exposed to the external laser field.

During photoionization (PI), tunneling ionization (TI) can be considered as an initial key process. Therefore, a detailed understanding of TI is necessary for the further understanding of strong-field physics of atoms and molecules. According to (KELDYSH, 1965), the choice of the governing PI mechanism is dictated by the famous Keldysh parameter, γ. TI is a limiting case of PI for the value of the Keldysh parameter much less than unity, $\gamma = \frac{\omega\sqrt{2I_p}}{F} \ll 1$, where I_p is ionization potential, ω frequency and F the strength of the field. Although analysis and

understanding of the physical processes associated with TI are progressing fast, complete, and detailed modeling of the mechanisms is still an open scientific topic. In the opposite limit, $\gamma \gg 1$, the electron is ionized from the molecule by absorbing several photons and this process is known as a multiphoton ionization (MPI). The intermediate regime ($\gamma \sim 1$) is intuitively considered as the borderline between the TI and MPI depending on laser field parameters.

Molecules are much more difficult systems for modeling than atoms due to their complex dynamic. Nevertheless, the values for TI rates of atoms and molecules with approximately the same ionization potential and nearly identical binding energies are usually close to each other (TONG *et al.*, 2002). Tong and his coworkers in (TONG *et al.*, 2002) investigated the ionization of molecules versus atoms while presenting a novel theoretical model (so-called MO-ADK) for calculating the ionization rates of diatomic molecules. According to (ZHAO *et al.*, 2011; GONG *et al.*, 2017), their model can be successfully extended to triatomic and polyatomic molecules.

In this paper, we investigated the photoionization rates and yields of ammonia molecule (NH_3) using non–perturbative approach. We analyzed numerically and analytically the influence of the magnetic field component on the tunneling yield, in a strong near-relativistic field. We choose ammonia molecule because it is simple enough for our calculations, but also for following reasons. As demonstrated recently, its properties such as diffusivity, viscosity, and structure have a considerable impact on the internal evolution and magnetic field of giant planets (ROBINSON *et al.*, 2017). The increase of ammonia molecule emissions in the atmosphere has negative influence on climate change, environmental and public health. This is why the number of research papers related to NH_3 emissions into the atmosphere increased over the previous year (WANG *et al.*, 2020; LI *et al.*, 2020).

THEORETICAL BACKGROUND

The first attempt to determine molecule transition rate was classical, the adiabatic Ammosov-Delone-Krainov model (ADK) (AMMOSOV *et al.*, 1986) which had limited success. The problem was that the ADK ionization model often overestimates the ionization rates thereby shifting saturation intensities to lower values for many molecules. That is why, sixteen years later, the ADK theory is upgraded for molecules, and the MO-ADK is obtained (TONG *et al.*, 2002). The main improvement is the incorporation of molecular orbitals. The characteristic exponential dependence of transition rate on the field intensity, F, and the ionization potential, I_p is kept (TONG *et al.*, 2002):

$$W_{MO-ADK}(F,R) = \sum_{m'} \frac{|B(m')|^2}{2^{|m'|}|m'|!} \frac{1}{k^{2n^*-1}} \left(\frac{2k^3}{F}\right)^{2n^*-|m'|-1} \times \mathrm{Exp}\left[-\frac{2k^3}{F}\right], \quad (1)$$

where m is the magnetic quantum number along the molecular axis, l and n^* are the angular and the effective principal quantum numbers, $n^* = \frac{Z_C}{k}$ (here Z_C denotes the effective Coulomb charge and k is the characteristic momentum of the bound state, $\kappa = \sqrt{2I_p}$). Next, $B(m')$ is defined as $B(m') = \sum_{l,m} C_{n^*l}\, D^l_{m',\,m}(\phi,\theta,\chi) Q(l,m')$, where C_{n^*l} and $Q(l,m)$ are the structure coefficients of the given molecule, defined as: $C_{n^*l} = \left(\frac{2e}{n^*}\right)^{n^*} \frac{1}{\sqrt{2\pi n^*}}$ and $Q(l,m) = (-1)^m \left[\frac{((2l+1)(l+|m|)!)}{(2(l-|m|)!)}\right]^{\frac{1}{2}}$. In addition, $D^l_{m',m}(\phi,\theta,\chi)$ denotes Wigner's rotation matrix, where (ϕ,θ,χ) are the Euler angles. The rotation around the molecular z axis is represented by χ, and θ represents the azimuthal angle, while the angle of rotation around the polarization vector is, ϕ, and for linearly polarized lasers is fixed to 0. The linearly polarized

laser field is assumed. Atomic units, $m = e = \hbar = 1$, are used through the paper (SHULL and HALL, 1959).

In order to determine Wigner's rotation matrix, it is convenient to introduce rotation operator, $\hat{R}_n(\alpha) = \exp(-\mathrm{i}\alpha \mathrm{J}\hat{\mathrm{n}})$, where α is an arbitrary angle, and $\mathrm{J}\hat{\mathrm{n}} = -i\frac{\partial}{\partial\alpha}$ is projection of angular momentum J on arbitrary axis (YAMANI AND FISHMAN, 2008). For the Euler angles, rotation operator becomes (ZARE, 1988):

$$\widehat{R}(\phi,\theta,\chi) = \mathrm{Exp}\left[-i\chi J\hat{n}_\chi\right]\mathrm{Exp}[-i\theta J\hat{n}_\theta]\mathrm{Exp}\left[-i\phi J\hat{n}_\phi\right]. \tag{2}$$

Now, Eq. (2) can be rewritten as the following:

$$R(\phi,\theta,\chi)|lm\rangle = \sum_{m'} D^l_{m',\ m}(\phi,\theta,\chi)|lm'\rangle. \tag{3}$$

By projecting the equation from the left with $\langle lm'|$ and using the orthonormality of the angular momentum states, $\langle \Phi_i|\Phi_j\rangle = \delta_{ij}$, we found an explicit expression for the Wigner's rotation matrix elements (ZARE, 1988):

$$D^l_{m',\ m}(\phi,\theta,\chi) = \langle lm'|R(\phi,\theta,\chi)|lm\rangle, \tag{4}$$

where the Wigner's matrix, $R(\phi,\theta,\chi)$, is a matrix of dimension $(2J+1)\times(2J+1)$. Because we are interested in examining the ionization rate along the z-axis, the matrix elements presented using Eq. (4) can be found using the following expressions: $D^l_{m',m}(\phi,\theta,\chi) = \mathrm{Exp}[-i\phi m']d^l_{m',m}(\theta)\mathrm{Exp}[-i\chi m]$, where $d^l_{m',m}(\theta) = \langle lm'|e^{-il\theta}|lm\rangle$ denotes the element of the orthogonal Wigner's (small) d-matrix.

Based on the results presented in (WIGNER, 1931) d −matrix element $d^l_{m',\ m}(\theta)$, can be derived using the following series expression:

$$d^l_{m',\ m}(\theta) = \sqrt{\frac{(l+m')!(l-m')!}{(l+m)!(l-m)!}}\sum_s(-1)^{m'-m+s}\binom{l+m}{s}\binom{l-m}{l-m'-s}\times \\ \times\left(\cos\frac{\theta}{2}\right)^{2l+m-m'-2s}\left(\sin\frac{\theta}{2}\right)^{m'-m+2s}, \tag{5}$$

where $\binom{l+m}{s}$ and $\binom{l-m}{l-m'-s}$ are binomial coefficients. The summation over parameter s is only restricted to the argument of any factorial which is non-negative.

Using Eq. (5) we examined the symmetry properties of $d^l_{m',m}(\theta)$ for ammonia molecule, i.e., for the fixed values of $l = 2$, we varied m as $m[0,\ 1,\ 2]$. Using well known formula for the binomial coefficients: $\binom{\lambda}{l} = \frac{\lambda!}{l!(\lambda-l)!}$, and calculating $s = l - m' - \sigma$, ($\sigma = 0$ for amonia molecule), for $(l,m',m)\to(2,0,0)$, it follows: $d^2_{00}(\theta) = \sqrt{\frac{(2+0)!(2-0)!}{(2+0)!(2-0)!}}\times \sum_s(-1)^{0-0+s}\binom{2+0}{s}\binom{2-0}{2-0-s}\left(\cos\frac{\theta}{2}\right)^{2*2+0-0-2s}\left(\sin\frac{\theta}{2}\right)^{0-0+2s}$, i.e.

$$d^2_{00}(\theta) = \sum_s(-1)^s\binom{2}{s}\binom{2}{2-s}\left(\cos\frac{\theta}{2}\right)^{4-2s}\left(\sin\frac{\theta}{2}\right)^{2s}. \tag{6}$$

We made summation over s and obtained:

$$d^2_{00}(\theta) = \left(\cos\frac{\theta}{2}\right)^4 - 4\left(\cos\frac{\theta}{2}\right)^2\left(\sin\frac{\theta}{2}\right)^2 + \left(\sin\frac{\theta}{2}\right)^4 =$$

$$= \left(\cos\frac{\theta}{2}\right)^4 + 2\left(\cos\frac{\theta}{2}\right)^2\left(\sin\frac{\theta}{2}\right)^2 + \left(\sin\frac{\theta}{2}\right)^4 - 2\left(\cos\frac{\theta}{2}\right)^2\left(\sin\frac{\theta}{2}\right)^2 - (\sin\theta)^2 =$$
$$= \left(\left(\cos\frac{\theta}{2}\right)^2 + \left(\sin\frac{\theta}{2}\right)^2\right)^2 - \frac{(\sin\theta)^2}{2} - (\sin\theta)^2 =$$
$$= 1 - \frac{3(\sin\theta)^2}{2}. \quad (7)$$

After some trigonometric transformation, as a result, the final expression is obtained:

$$d^2_{00}(\theta) = \frac{1}{2}(3\cos^2[\theta] - 1). \quad (8)$$

Following the same recipe, the other coefficients can be calculated:

$$d^2_{11}(\theta) = \frac{1}{2}(2\cos[\theta] - 1)(\cos[\theta] + 1),\ d^2_{22}(\theta) = \cos^4\left[\frac{\theta}{2}\right]. \quad (9)$$

The abovementioned calculations of Wigner's rotation matrix provide a great accuracy for a wide range of atoms and molecules and are used to evaluate the ionization rates in the frame of both ADK and MO-ADK theories. To obtain a more accurate expression of the rate for the special case of ammonia molecule, we observed geometry optimization which leads to N–H bond length of 1.017 Å, while H–N–H bond angle is 107.8° (see (NILSSON, 2005)). In this case, as one can see from Figure 1, its molecule has a pyramidal shape forming an oscillating umbrella structure (See Fig. 1).

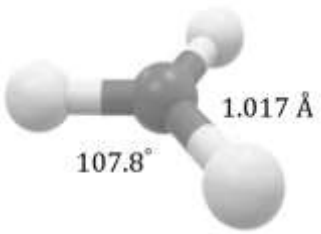

Figure 1. The geometry optimization of ammonia molecule (NILSSON, 2005).

In order to compare theoretical findings with experimental, it is convenient to calculate ionization yield, Y, because this quantity is usually measured in experiments. Its expression is directly related to the ionization rate, and dependent upon the laser electric field strength, F as (MILADINOVIĆ and PETROVIĆ, 2014):

$$Y_{MO-ADK}(F,R) = \int W_{MO-ADK}(F,R)\cdot dt. \quad (10)$$

Next we assumed a hyperbolic-secant-squared time distribution, $F(t) = F_0\mathrm{sech}^2\left(\frac{t}{\tau}\right)$ (AMMOSOV *et al.*, 1992), where τ is the pulse width at full width at half maximum (FWHM). For this time distribution, a relation for the ionization probability yield for ammonia molecule can be approximated by:

$$Y_{MO-ADK}(F,R,t) \propto Z_{l,m,m'}(R)\int \frac{1}{\mathrm{sech}^2\left(\frac{t}{\tau}\right)} \times \mathrm{Exp}\left[-\frac{2k^3}{F_0}\frac{1}{\mathrm{sech}^2\left(\frac{t}{\tau}\right)}\right]dt, \quad (11)$$

where $Z_{l,m,m'}(R) = \sum_{m'}\left(\frac{2k^3}{F_0}\right)^{2n^*-|m'|-1}\frac{\left|\sum_{l,m} C_{lm}\, D^l_{m',\ m}(R)Q(l,m')\right|^2}{2^{|m'|}|m'|!k^{2n^*-1}}$. The integral in Eq. (11) can be evaluated using an expansion in terms of quadratic hyperbolic secant function as in (https://functions.wolfram.com/ElementaryFunctions/Sech/06/02/):

$$\mathrm{sech}^2\left(\frac{t}{\tau}\right) = 4\left(\sum_{k=1}^{\infty}(-1)^k\, q^{2k-1}\right)^2, \quad (12)$$

where q can be expanded in exponential form as: $q = \mathrm{Exp}[x]$. The resulting integrals in Eq. (11) now have an analytical form, which may be written as:

$$Y_{MO-ADK}(F,R,t) \propto \frac{1}{4}\, Z_{l,m,m'}(R) \int \left(1-\left(\frac{t}{\tau}\right)^2\right)^{-2} \times \mathrm{Exp}\left[-\frac{k^3}{2F_0}\left(1-\left(\frac{t}{\tau}\right)^2\right)^{-2}\right] dt \,. \quad (13)$$

Eq. (13) can be computed by using the Taylor-series expansion methods for solving integral equations (HUABSOMBOON *et al.*, 2010). As a result the folowing equation can be obtained:

$$Y_{MO-ADK}(F,R,t) \propto \frac{1}{4}\, Z_{l,m,m'}(R) \left(\frac{t}{\tau}\right)\left\{1+\frac{2t^2\left(F_0-2k^3\right)}{3F_0\tau^2}\right\} \times \mathrm{Exp}\left[-\frac{k^3}{2F_0}\right]. \quad (14)$$

Theoretical and numerical investigations of the molecular ionization yields, based on the MO-ADK model, have been usually performed without the inclusion of the effect of the magnetic component of laser radiation. Magnetic component contributes to the ion yield through Lorentz ionization only in the near-relativistic regime, and in the following, we have included it into our analysis.

For the relativistic intensities of electromagnetic radiation, the MO-ADK expression, $W_{MO-ADK}(F,R)$, with the correction for nonzero initial momentum, p, of the photoelectron has the following form (DELONE *et al.*, 1993):

$$W^{rel}_{MO-ADK}(F,R) = W_{MO-ADK}(F,R) \times \mathrm{Exp}\left[-\frac{2E_e{\gamma^{rel}}^3}{3\omega} - \frac{{E_e}^2\gamma^{rel}}{c^2\omega}\right], \quad (15)$$

where E_e is the relativistic kinetic energy of ejected photoelectrons defined as in (KRAINOV, 1998): $E_e = \sqrt{p^2c^2+c^4} - c^2$. Here c denotes the speed of light in atomic units, $c = 137.02$, and p is the momentum of ejected photoelectrons. It is important to note that under the frame of tunneling theory, the magnetic effects set a lower limit on Keldysh adiabaticity parameter. According to (MILADINOVIĆ and PETROVIĆ, 2015) the condition $\gamma \to 0$ represents an extreme relativistic limit. In that case, the relativistic Keldysh parameter, γ^{rel}, must be introduced: $\gamma^{rel} = \frac{\omega c\sqrt{1-\left[\frac{\left(c^2-\frac{Z^2}{2}\right)}{c^2}\right]^2}}{F}$, where Z is the ion charge.

For purpose of incorporating the magnetic component of the laser field in the near-relativistic transition rate, we shall extend Eq. (15) using the definition of the Lorentz ionization rate (ZHAKENOVICH *et al.*, 2015):

$$W^{rel}_{M}(F,R) = S\sqrt{1-v^2}\, W^{rel}_{MO-ADK}(F,R), \quad (16)$$

where v is the electron velocity and S is the stabilization factor.

By implementing the equation for Lorentz transition rate (Eq. (16)) into already defined expression for the ion yield, $Y^{rel}_{M}(F,R) = \int W^{rel}_{M}(F,R)\cdot dt$, we obtained:

$$Y^{rel}_{M}(F,R,t) = S\, Z_{l,m,m'}(R)\sqrt{1-v^2}\int \frac{\mathrm{Exp}\left[-\frac{2k^3}{F_0\,\mathrm{sech}^2\left(\frac{t}{\tau}\right)}\right]}{\mathrm{sech}^2\left(\frac{t}{\tau}\right)} \times$$
$$\times \mathrm{Exp}\left[-\frac{2E_e}{3\omega}\left[\frac{\omega c\sqrt{1-\left[\frac{c^2-\frac{Z^2}{2}}{c^2}\right]^2}}{F_0\,\mathrm{sech}^2\left(\frac{t}{\tau}\right)}\right]^3 - \frac{{E_e}^2}{c^2\omega}\left[\frac{\omega c\sqrt{1-\left[\frac{c^2-\frac{Z^2}{2}}{c^2}\right]^2}}{F_0\,\mathrm{sech}^2\left(\frac{t}{\tau}\right)}\right]\right] dt \,. \quad (17)$$

Eq. (17) cannot be solved analytically due to the complex integral representation. Because of that, the ion yield obtained at near-relativistic field intensities while including the magnetic field component (Eq. (17)), must be solved numerically.

RESULTS AND DISCUSSION

We considered ammonia, NH_3, molecule, in the linearly polarized laser field, with a hyperbolic-secant-squared time distribution, using the MO-ADK theoretical approach. We observed the ionization of ammonia through tunneling of electrons from the highest occupied molecular orbital, with γ in a range covering from 0.025 to 0.8. The laser field intensity varied within the range $10^{13} < I < 10^{17}$ Wcm^{-2}. We used laser wavelenght $\lambda = 800$ nm.

First of all, we investigated the geometry-dependent ionization behavior of ammonia molecules. Analysis presented in Fig. 2 is especially important for the study of the nuclear motion in neutral ammonia (WILEY AND MCLAREN, 1955).

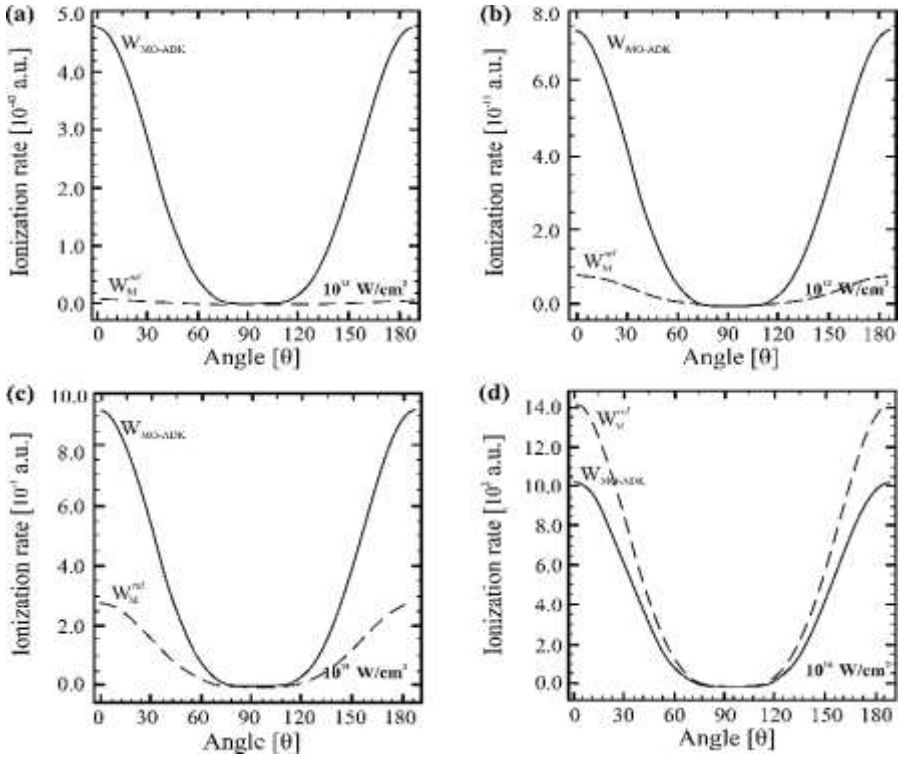

Figure 2. The orientation dependent ion rate for ammonia using MO-ADK theory, $W_{MO-ADK}(F,R)$ (solid lines), and the near-relativistic transition rate with incorporated magnetic component, $W_M^{rel}(F,R)$ (dashed lines), for fixed laser intensities of (a) $1 \times \frac{10^{13}\,\mathrm{W}}{\mathrm{cm}^2}$, (b) $1 \times \frac{10^{14}\,\mathrm{W}}{\mathrm{cm}^2}$, (c) $1 \times \frac{10^{15}\,\mathrm{W}}{\mathrm{cm}^2}$, and (d) $1 \times \frac{10^{16}\,\mathrm{W}}{\mathrm{cm}^2}$.

In Fig. 2, we presented the orientation-dependent ion rate for ammonia for the pure non-relativistic approach, $W_{MO-ADK}(F,R)$, and relativistic with the included effect of the magnetic component of the laser field, $W_M^{rel}(F,R)$. The graphs show increasing of the ion yield with the field intensity increasing and this behavior is in accordance with (SAYRES *et al.*, 2011). On the other hand, the curves behave differently and differ strongly with increasing the field intensity. Based on the presented results, one can conclude that inclusion of the magnetic component in the near-relativistic regime (when $I \geq 1 \times \frac{10^{16}\,\mathrm{W}}{\mathrm{cm}^2}$) of laser field strongly increase the value of the transition rate with field intensity rising and the near-relativistic transition rate with the

incorporated magnetic component $W_M^{rel}(F,R)$ is dominanting. These findings are completely expected and in accordance with (SMEENK *et al.*, 2011).

Next, we observed ammonia ionization yield. In order to validate the analytical solution given in Eq. 14, Eq. 13 was integrated numerically using Wolfram Mathematica scripts (WOLFRAM, 1999). The integral in Eq. 13 was discretized using the Laplace transform, $\int f(x)h(x)dx = \int f(x)(\sum_{n=1}^{\infty} u_n\, e^{-nx})dx = \sum_{n=1}^{\infty} u_n \int e^{-nx} f(x)\, dx = \sum_{n=1}^{\infty} u_n v_n$ (LESKO and SMITH, 2003). Our analytical and numerical calculations are presented in Fig. 3 and one can see a good agreement between analytical and numerical curve. It is also important to stress that ionization yields presented in Fig. 3 are for weak or non-relativistic fields and because of that can be linked to one of the previous equations (Eq. 13 for numerical solution and Eq. 14 for analytical solution).

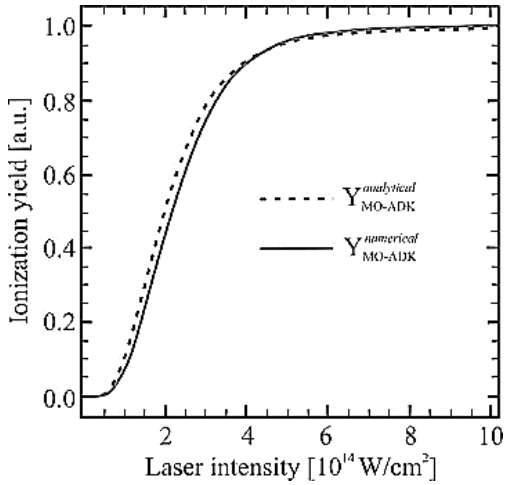

Figure 3. Numerically (solid line) and analytically (dashed line) (Eq. (15)) calculated ionization yields ($\lambda = 800$ nm) for the ammonia molecule using the MO-ADK model.

From Fig 2. follows that the MO-ADK prediction of the ionization yield is small at low intensities and reaches saturation, i.e. complete single ionization, at higher intensities, ($\sim 1 \times \frac{10^{15}\,\mathrm{W}}{\mathrm{cm}^2}$). This behaviour agrees with the results of (SAYRES *et al.*, 2011). The deviation can be seen near the critical value of the intensity threshold, $I_c[\mathrm{Wcm}^{-2}] = 4 \times \frac{10^9 I_p^4[\mathrm{eV}]}{Z^2}$ (HUSSIEN, 2015), which in our study denotes $I_c = 4.96 \times 10^{14}\ \mathrm{Wcm}^{-2}$. This deviation is totally expected as a number of theories break down in this region.

In the near relativistic field intensities region, $10^{16} < I < 10^{17}\ \mathrm{Wcm}^{-2}$, we investigated the influence of magnetic field component on the total ammonia yield. For this purpose, we compared results for relativistic ion yield without, $Y^{rel}(F,R)$ (Eq. 10), and with correction of the magnetic field, $Y_M^{rel}(F,R,t)$ (Eq. 17). Results are presented in Fig. 4.

Fig. 3, shows that for the lower laser field intensities region, both curves, the one which includes correction of the magnetic field $Y_M^{rel}(F,R,t)$ and the other which neglect the magnetic field component $Y^{rel}(F,R)$, have almost the same flow. But with the intensity increasing, there is a deviation between curves. One can see that for $I < 0.5 \times 10^{16}\ \mathrm{Wcm}^{-2}$, both curves sharply rise together, but with field increase, $Y^{rel}(F,R)$, for the same field intensities have the higher values then $Y_M^{rel}(F,R,t)$. On $I = 6.53 \times \frac{10^{16}\,\mathrm{W}}{\mathrm{cm}^2}$ both, $Y^{rel}(F,R)$ and $Y_M^{rel}(F,R,t)$, have the same values. Starting from there one can see that separation between curves increases with intensity. A curve that represents pure relativistic rate tends to remain nearly saturated, while the other curve represents rate with considering the magnetic component. Based on graphs, it is obvious that the transition rate is affected by the magnetic component of the laser field. In

other words, our results simply show that the dependence of the magnetic component is not significant enough for lower field intensities and, on the other hand, that it is significant for higher regions. This finding is in accordance with (DELIBAŠIĆ *et al.*, 2018).

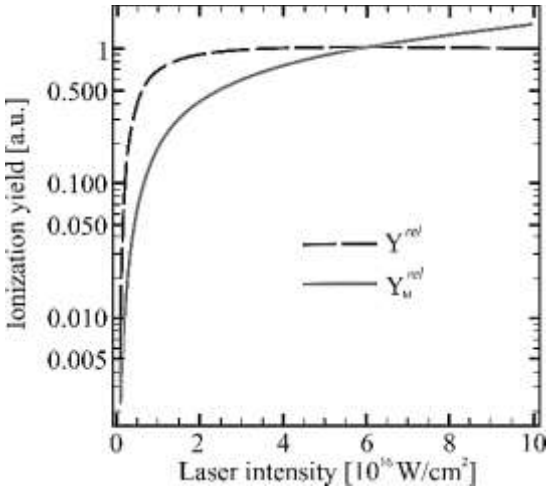

Figure 4. A comparative review of the ammonia ionization yields without, $Y^{rel}(F,R)$ (dashed line), and with correction of the magnetic field, $Y_M^{rel}(F,R,t)$ (solid line). Field intensity varies within the range $10^{16} < I < 10^{17}$ Wcm^{-2}.

CONCLUSION

In summary, we have investigated the influence of the magnetic component of the laser field on the photoionization yield of the ammonia molecule. We showed that, in the near-relativistic intensities, magnetic component has a strong contribution to the yield and should be taken into account. Our results indicate that this contribution increases with field intensities. Our findings are in a good agreement with available theoretical results.

Acknowledgments

This work was supported by the Serbian Ministry of Education, Science and Technological Development (Agreement No. 451-03-9/2021-14/200122) and COST Action CA18222 “Attosecond Chemistry”.

References:

[1] AMMOSOV, M. V., DELONE, N. B., KRAINOV, V. P. (1986): Tunnel Ionization of Complex Atoms and Atomic Ions in Electromagnetic Field. *High Intensity Laser Processes.* doi:10.1117/12.938695

[2] AMMOSOV, M.V., GOLOVINSKY, P.A., KIYAN, I.Y., KRAINOV, V.P., RISTIC, V.M. (1992): Tunneling ionization of atoms and atomic ions in an intense laser field with a nonhomogeneous space–time distribution. *JOSA B* **9** (8):1225-1230.

[3] ARNOLD, C., VENDRELL, O., SANTRA, R. (2017): Electronic decoherence following photoionization: Full quantum-dynamical treatment of the influence of nuclear motion. *Physical Review A* **95** (3): 033425. doi: 10.1103/PhysRevA.95.033425

[4] BRAY, A.W., FREEMAN, D., ECKART, S., KHEIFETS, A.S. (2019): Correlation enhancement of high-order harmonic generation in Xe. *Physical Review A* **100** (1): 013404. doi: 10.1103/PhysRevA.100.013404

[5] BRENNECKE, S. AND LEIN, M. (2018): High-order above-threshold ionization beyond the electric dipole approximation. *Journal of Physics B: Atomic, Molecular and Optical Physics* **51** (9): 094005. doi:10.1088/1361-6455/AAB91F

[6] CHANG, Y.C., LIU, K., KALOGERAKIS, K.S., NG, C.Y., JACKSON, W.M. (2019): Branching Ratios of the N (2D03/2) and N (2D05/2) Spin–Orbit States Produced in the State-Selected Photodissociation of N2 Determined Using Time-Sliced Velocity-Mapped-Imaging Photoionization Mass Spectrometry (TS-VMI-PI-MS). *The Journal of Physical Chemistry A* **123** (12): 2289-2300. doi: 10.1021/acs.jpca.8b11691

[7] DELIBAŠIĆ, H., ISAKOVIĆ, K., PETROVIĆ, V., MILADINOVIĆ, T. 2018. Estimation of the Influence of the Magnetic Component on the Transition Rate in a Linearly Polarized Laser Field. *International Journal of Theoretical Physics* **57** (2): 406-413. doi: 10.1007/s10773-017-3572-7

[8] DELONE, N.B., KIYAN, I.Y., KRAINOV, V.P. (1993): Ionization of atoms by a strong low-frequency field. *Laser Physics* **3** (2): 312-322.

[9] GONG, X., LI, H., LU, P., SONG, Q., JI, Q., LIN, K., ZHANG, W., MA, J., LI, H., ZENG, H., WU, J. (2017): Ellipticity dependent symmetric break of doubly ionized acetylene in strong laser fields. *Journal of Optics* **19** (12): 124008. doi: 10.1088/2040-8986/aa938f

[10] HUABSOMBOON, P., NOVAPRATEEP, B., KANEKO, H. (2010): On Taylor-series expansion methods for the second kind integral equations. *Journal of computational and applied mathematics* **234** (5): 1466-1472. doi: 10.1016/j.cam.2010.02.023

[11] HUSSIEN, A.M.M. (2015): Ionization of diatomic molecules in intense laser fields. *PhD thesis*, Mathematisch-Naturwissenschaftlichen Fakultät der Humboldt-Universität zu Berlin. [in Germany]

[12] KELDYSH, L.V. (1965): Ionization in the field of a strong electromagnetic wave. *Sov. Phys. JETP* **20** (5): 1307-1314.

[13] KRAINOV, V.P. (1997): Ionization rates and energy and angular distributions at the barrier-suppression ionization of complex atoms and atomic ions. *JOSA B* **14** (2): 425-431.

[14] KRAINOV, V.P. (1998): Energy distribution of relativistic electrons in the tunneling ionization of atoms by super-intense laser radiation. *Optics express* **2** (7): 268-270.

[15] LESKO, J.P. and SMITH, W.D. (2003): A Laplace transform technique for evaluating infinite series. *Mathematics magazine* **76** (5): 394-398.

[16] LI, S., SIERRA-COSTA, D., MICHIE, M.J., BEN-ITZHAK, I., DANTUS, M. (2020): Control of electron recollision and molecular nonsequential double ionization. *Communications Physics* **3** (1): 1-8. doi: 10.1038/s42005-020-0297-3

[17] LI, X., XU, J., JIANG, Y., HE, Z., LIU, B., XIE, H., LI, H., LI, Z., WANG, Y., TAI, H. (2020): Toward agricultural ammonia volatilization monitoring: A flexible polyaniline / Ti3C2Tx hybrid sensitive films based gas sensor. *Sensors and Actuators B: Chemical*, **316**: 128144. doi: 10.1016/j.snb.2020.128144

[18] MILADINOVIĆ, T.B. AND PETROVIĆ, V.M. (2014): Quasiclassical approach to tunnel ionization in the non-relativistic and relativistic regimes. *Revista mexicana de física* **60** (4): 290-295.

[19] MILADINOVIĆ, T.B. AND PETROVIĆ, V.M. (2015): Relativistic Angular Distribution of Photoelectrons in the Tunneling Ionization of Atoms by a Linearly Polarized Laser Field. *Brazilian Journal of Physics* **45** (2): 251-257. doi: 10.1007/s13538-015-0303-5

[20] NILSSON, K.B. (2005): Coordination chemistry in liquid ammonia and phosphorous donor solvents. *PhD thesis*, Acta Universitatis Agriculturae Sueciae, (21): 1652-6880. Uppsala: Sveriges lantbruksuniv.

[21] PENG, P., MARCEAU, C., VILLENEUVE, D.M. (2019): Attosecond imaging of molecules using high harmonic spectroscopy. *Nature Reviews Physics* **1** (2): 144-155. doi: 10.1038/s42254-018-0015-1

[22] ROBINSON, V.N., WANG, Y., MA, Y., HERMANN, A. (2017): Stabilization of ammonia-rich hydrate inside icy planets. *Proceedings of the National Academy of Sciences* **114** (34): 9003-9008. doi: 10.1073/pnas.1706244114

[23] SAYRES, S.G., ROSS, M.W., CASTLEMAN, A.W. (2011): Influence of clustering and molecular orbital shapes on the ionization enhancement in ammonia. *Physical Chemistry Chemical Physics* **13** (26): 12231-12239. doi: 10.1039/C1CP20612E

[24] SHULL, H., AND HALL, G.G. (1959): Atomic units. *Nature* **184** (4698): 1559-1560.

[25] SMEENK, C.T.L., ARISSIAN, L., ZHOU, B., MYSYROWICZ, A., VILLENEUVE, D.M., STAUDTE, A., CORKUM, P.B. (2011): Partitioning of the linear photon momentum in multiphoton ionization. *Physical review letters* **106** (19): 193002. DOI: 10.1103/PhysRevLett.106.193002

[26] TONG, X.M., ZHAO, Z.X. AND LIN, C.D., (2002): Theory of molecular tunneling ionization. *Physical Review A* **66** (3): 033402.

[27] WANG, M., KONG, W., MARTEN, R., HE, X.C., CHEN, D., PFEIFER, J., HEITTO, A., KONTKANEN, J., DADA, L., KÜRTEN, A. AND YLI-JUUTI, T. (2020): Rapid growth of new atmospheric particles by nitric acid and ammonia condensation. *Nature* **581** (7807): 184-189. doi: 10.1038/s41586-020-2270-4

[28] WIGNER, E.P. (1931): Gruppentheorie und ihre Anwendung auf die Quantenmechanik der Atomspektren. pp. 332. ISBN: 978-3-663-02555-9.

[29] WILEY, W.C. AND MCLAREN, I.H. (1955): Time-of-flight mass spectrometer with improved resolution. *Review of scientific instruments* **26** (12): 1150-1157.

[30] WOLFRAM, S. (1999): The MATHEMATICA® book, version 4. Cambridge university press.

[31] YAMANI, H.A. AND FISHMAN, L. (2008): J-Matrix Method: Extensions to Arbitrary Angular Momentum and to Coulomb Scattering. *In*: Alhaidari A.D., Yamani H.A., Heller E.J., Abdelmonem M.S. (eds) *The J-Matrix Method*. Springer, Dordrecht. doi: 10.1007/978-1-4020-6073-1_2.

[32] YUAN, K.J., LU, H., BANDRAUK, A.D. (2017): Photoionization of triatomic molecular ions by intense bichromatic circularly polarized attosecond UV laser pulses. *Journal of Physics B: Atomic, Molecular and Optical Physics* **50** (12): 124004. doi: 10.1088/1361-6455/aa72fa

[33] ZARE, R.N. (1988): Angular momentum. *Understanding Spatial Aspects in Chemistry and Physics.* Baker Lecture Seriespp, Wiley. pp 368. ISBN: 978-0-471-85892-8

[34] ZHAKENOVICH, A.E., VALENTINA, Y., NESSIPBAY, T., TATYANA, S., ZHADYRA, Y. (2015): Effect of Magnetic Field on the Ionization Potential of the Atoms and Ions. *Journal of Chemistry and Chemical Engineering* **9**: 299-302. doi: 10.17265/1934-7375/2015.04.009

[35] ZHAO, S.F., LIU, L., ZHOU, X.X. (2014): Multiphoton and tunneling ionization probability of atoms and molecules in an intense laser field. *Optics Communications* **313**: 74-79. doi: 10.1016/j.optcom.2013.09.074

[36] ZHAO, S.F., XU, J., JIN, C., LE, A.T., LIN, C.D. (2011): Effect of orbital symmetry on the orientation dependence of strong field tunnelling ionization of nonlinear polyatomic molecules. *Journal of Physics B: Atomic, Molecular and Optical Physics* **44** (3): 035601. doi:10.1088/0953-4075/44/3/035601

[37] https://functions.wolfram.com/ElementaryFunctions/Sech/06/02/